

GTFR-102

**PHYSICS MODELS AND USER'S GUIDE
FOR THE NEUTRAL BEAM MODULE OF THE
SUPERCODE**

John Mandrekas

**Fusion Research Center
Georgia Institute of Technology
Atlanta, GA 30332-0225**

August, 1992

1. INTRODUCTION

This report contains a description of the neutral beam heating and current drive module **Beams**, that was developed at Georgia Tech for the SUPERCODE, the new systems and operations code for the ITER EDA [1]. The NB module calculates profiles of the neutral beam deposition, fast ion pressure, beam heating power, and neutral beam driven current density. It also computes global parameters such as current drive efficiencies, beam shinethrough, fast beam ion beta, and the fusion power and neutron production due to beam-plasma interactions.

The most important consideration during the development of this module was to make it computationally fast without compromising physical accuracy. We believe that through careful selection of physical models and optimized coding, these conflicting requirements have been largely met. As a result, the SuperCode has now the ability to perform self-consistent calculations involving NB heating and current drive. This capability is very important for the study of sub-ignited, hybrid, or steady-state ITER and post-TFTR reactor operating scenarios. It is also the first time that a systems code has had such capabilities, usually found only in 1½-D plasma transport codes.

2. PHYSICAL MODELS

2.1. Deposition Profiles

The first step in any computation involving neutral beam injection in a plasma, is the calculation of the neutral beam deposition profile: As the fast atoms enter the plasma, they become ionized through interactions with the background electrons and ions (electron impact ionization, ion impact ionization, charge exchange). The number of atoms ionized within the toroidal volume element $V'(\rho)d\rho$ is equal to:

$$\frac{I_0/e}{V_p} H(\rho) V'(\rho) d\rho \quad (1)$$

where I_0 is the (atomic equivalent) injection current in A, V_p is the plasma volume, and $H(\rho)$ is the NB deposition profile¹. Therefore, the fast ion source in the plasma due to the NB injection is:

$$\dot{n}_f(\rho) \left(\frac{\#ions}{m^3 s} \right) = \frac{I_0/e}{V_p} H(\rho) \quad (2)$$

¹ For systems based on positive-ion sources, each beamline has three energy components (E , $E/2$, $E/3$) and therefore three different deposition profiles are calculated.

Several techniques are available for the calculation of the NB deposition profile $H(\rho)$ in toroidal plasmas. They are based either on Monte Carlo methods [2], or on some type of pencil-beamlet techniques [3,4]. The model chosen for the SUPERCODE is based on the diffuse-beam model developed by Rome *et al* [3]. The model is computationally fast while retaining most of the important physics, and it is *exact* for midplane injection in a tokamak plasma with shifted elliptical flux surfaces of variable elongation. The SUPERCODE implementation of the model is similar to that found in the PROCTR transport code [5], but extended to allow flux surfaces with variable elongation, and beams with rectangular cross sections and different power distributions.

According to the diffuse beam model, the deposition profile due to a beamlet with tangency radius R_b and distance above the midplane Z_b is [5]:

$$h^\pm(\rho, R_b, Z_b) = \frac{2\rho V_p}{V'(\rho)} \frac{1}{\lambda(\rho)} \frac{R_\pm}{\sqrt{R_\pm^2 - R_b^2}} \left\{ \frac{1 + \frac{\kappa'(\rho)}{\rho} \frac{Z_b^2}{\kappa^3(\rho)} \pm \frac{\Delta'(\rho)}{\rho}}{\sqrt{\rho^2 - \frac{Z_b^2}{\kappa^2(\rho)}}} \right\} \left\{ \exp(-D_0) + \gamma_d \exp[-(D_0 + 2D_1)] \right\} \quad (3)$$

In the expression above, $\lambda(\rho)$ is the mean free path of the neutral beam ions in the plasma as a function of the flux surface label ρ (assumed to be equal to the midplane radius here), and is equal to $1/(n_e \sigma_{eff})$ where σ_{eff} is the effective beam stopping cross section which is calculated using the latest fits by C. Boley [6,7] that are valid for any plasma parameters and beam energies between 10 - 10,000 keV. The quantities $\kappa(\rho)$ and $\Delta(\rho)$ are the MHD elongation and plasma shift profiles, while a prime ' denotes the derivative $d/d\rho$. The quantity R_\pm represents the two possible intersections of the pencil beam with the flux surface with label ρ , the plus sign corresponding to the outer intersection and the minus sign to the inner one. For shifted elliptical cross sections with variable elongation we have,

$$R_\pm = R_0 + \Delta(\rho) \pm \sqrt{\rho^2 - \frac{Z_b^2}{\kappa^2(\rho)}} \quad (4)$$

if the intersection exists (i.e. if the term in the square root is positive.) The quantities D_0 and D_1 describe the attenuation of the beamlet along its optical path:

$D_0 \equiv D(R_{\pm}, R_{in})$, and $D_1 \equiv D(R_b, R_{\pm})$, where:

$$D(R_1, R_2) \equiv \int_{R_1}^{R_2} \frac{R dR}{\sqrt{R^2 - R_b^2}} \frac{1}{\lambda(\rho')} \quad (5)$$

R_{in} is the major radius at the first entrance of the beamlet into the plasma at the plane Z_b which, for our model, is equal to $R_0 + (a^2 - Z_b^2 / \kappa_a^2)^{1/2}$ where a is the minor radius. Notice that inside the integrand of D , the mean free path $\lambda(\rho)$ must be calculated at the flux surface ρ' that corresponds to the major radius R . This is found by solving the following nonlinear equation for ρ ,

$$\rho^2 = [R - (R_0 + \Delta(\rho))]^2 + \frac{Z_b^2}{\kappa^2(\rho)} \quad (6)$$

Finally, the parameter γ_d is equal to one if the beamlet intersects a given flux surface twice (double pass).

The expression for $h^{\pm}(\rho, R_b, Z_b)$ above, is for a pencil beam. To find the deposition profile for a beam with a finite cross section we would have to integrate the above result over the face of the beam, taking into account its shape and power density distribution within its cross-section. Therefore, the total deposition profile for the flux surface with label ρ including the contributions from the outer and inner intersections would be,

$$H(\rho) = H^+(\rho) + H^-(\rho)$$

where,

$$H^{\pm}(\rho) = 2 \int_0^{Z_u} dZ_b \int_{R_L}^{R_u} dR_b J_b(R_b, Z_b) h^{\pm}(\rho, R_b, Z_b) \quad (7)$$

We have made the assumption of up-down symmetry, so we only have to evaluate the integral for the upper half of the plasma cross section, resulting to the factor of 2 in front of the expression above. The integration limits Z_u, R_L , and R_u , as well as the current (or power) distribution function within the beam cross section, $J_b(R_b, Z_b)$, depend on the shape of the beam. Two different options for the beam shape are available, circular and rectangular, and for each shape we can have either uniform power distribution or a distribution with Gaussian shape.

Circular Beam:

The cross section shape of the finite beam is a circle of radius r_b . For a uniform current distribution within the beam cross section, $J_b(R_b, Z_b) = C$, where $C = 1/\pi r_b^2$ (normalization constant). For a Gaussian current distribution we have,

$$J_b(R_b, Z_b) = C \exp(-r^2/\sigma_R^2), \text{ for } r \leq r_b \quad (8)$$

where σ_R is the radial Gaussian half-width and $r = [Z_b^2 + (R_t - R_b)^2]^{1/2}$ with R_t being the beam tangency radius. The normalization constant C is determined from the requirement $2\pi \int_0^{r_b} J_b(r) r dr = 1$ and is equal to:

$$C = \frac{1}{\pi \sigma_R^2 (1 - \exp(-r_b^2/\sigma_R^2))} \quad (9)$$

The integration limits in the case of a circular beam are:

$$\begin{aligned} Z_u &= \min[\rho \kappa(\rho), r_b], \\ R_L &= R_t - \sqrt{r_b^2 - Z_b^2}, \text{ and} \\ R_u &= \min[R_\pm, R_t + \sqrt{r_b^2 - Z_b^2}] \end{aligned} \quad (10)$$

Rectangular Beam:

The shape of the beam cross section here is a rectangle with height h and width w . The current distribution function for a uniform distribution is $J_b(R_b, Z_b) = 1/wh$. In order to be able to model off-axis deposition, a bi-Gaussian distribution function is also available. For this, the function $J_b(R_b, Z_b)$ has the form,

$$J_b(R_b, Z_b) = C \exp\left(-\left(\frac{R_b - R_t}{\sigma_R}\right)^2\right) \left\{ \exp\left(-\left(\frac{Z_b - Z_s}{\sigma_Z}\right)^2\right) + \exp\left(-\left(\frac{Z_b + Z_s}{\sigma_Z}\right)^2\right) \right\} \quad (11)$$

where R_t is the beam tangency radius, Z_s is the position above the midplane of the peak of the distribution, and σ_Z is the Gaussian half-width in the vertical direction. The normalization constant C is equal to:

$$C = \frac{1}{\sigma_R \sigma_Z \pi \operatorname{erf}\left(\frac{w}{2\sigma_R}\right) \left\{ \operatorname{erf}\left(\frac{h - 2Z_s}{2\sigma_Z}\right) + \operatorname{erf}\left(\frac{h + 2Z_s}{2\sigma_Z}\right) \right\}} \quad (12)$$

The integration limits in the case of the rectangular beam are:

$$\begin{aligned}
Z_u &= \min[\rho\kappa(\rho), h/2], \\
R_L &= R_t - w/2, \text{ and} \\
R_u &= \min[R_{\pm}, R_t + w/2]
\end{aligned}
\tag{13}$$

This bi-Gaussian power distribution gives our model a considerable degree of flexibility in modeling different injection geometries. For $Z_s = 0$, we have the case of a rectangular beam with a centerline lying on the midplane. If however $Z_s \neq 0$, we can model off-axis injection with a symmetric configuration of two rectangular beamlines having centerlines above and below the midplane. Comparisons with the Monte Carlo NB deposition code NFREYA indicate that with the proper choice of Z_s and σ_z we can even model off-midplane injection at an angle with respect to the midplane, like the reference CDA case for ITER [8].

Beam shinethrough

Since the deposition profile is equal to the fraction of fast ions deposited in a given flux surface, it follows that the *beam shinethrough* f_s , i.e. the fraction of the total injected neutrals that were not ionized in the plasma, would be equal to:

$$f_s = 1 - \frac{1}{V_p} \int d\rho V'(\rho) H(\rho) \tag{14}$$

After the calculation of the shinethrough, the deposition profile $H(\rho)$ is normalized so that its volume integral over the plasma is equal to the plasma volume.

Limitations of the model

The deposition profile calculated with this implementation of the diffuse-beam model, is exact for midplane injection into a plasma with flux surfaces described by shifted ellipses of variable elongation (i.e. the triangularity of the flux surfaces is neglected). Only then it is possible to derive the quasi-analytic expressions described in this section. However, this limitation is not as serious as one might think. Unless the beams are aimed at the extreme outer part of the plasma near the X-ponts, the departure from the exact MHD geometry is small as it can be seen from Figure 1.

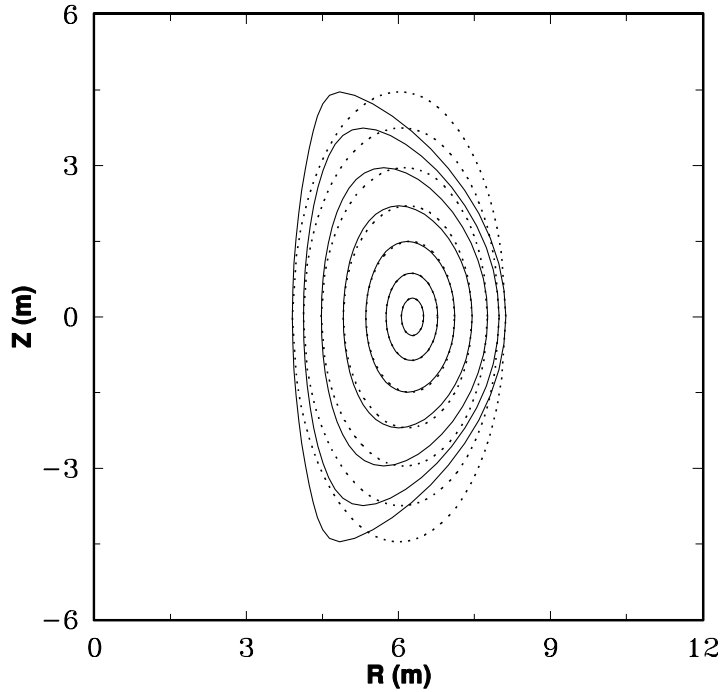


Figure 1: Comparison of flux surface geometries between the shifted ellipses with variable elongation model (dotted line) and the exact MHD geometry (solid line), for the ITER CDA.

Another limitation² of the model is its restriction to beamlines with axes lying on the midplane. However, as it was discussed above and will be demonstrated in following sections, we can get around this limitation, at least for beams of rectangular shape, by using the bi-Gaussian power distribution option.

The model cannot take into account the detailed optics of the injection system (beam focusing, beam divergence, beamline aperture considerations). These effects can be included in an average sense, by an appropriate choice of the Gaussian half-widths in the power distribution expressions.

Finally, the deposition profile calculated by this model is strictly speaking the *birth* profile of the fast ions. The actual deposition profile would differ due to first orbit effects. Here, we are making the assumption that first orbit effects are negligible and the fast ions slow down on their birth flux surface.

²Strictly speaking, this is not an inherent limitation of the model but rather a choice of the present implementation, to avoid having to integrate over the entire plasma cross section. Injection above (but still parallel to) the midplane can be modeled if we abandon the up-down symmetry assumption.

In spite of these limitations, the predictions of this semi-analytic deposition model agree surprisingly well with calculations performed with more accurate, but computationally expensive deposition codes. Several comparisons and benchmarks will be presented in following sections of this report.

2.2. Heating and Current Drive

Once the neutral beam deposition profile is known, a number of beam-related quantities can be evaluated. In this section the models for the beam heating and current drive are described.

Beam heating:

The NB plasma *absorbed* heating profile, assuming instantaneous thermalization, is given by the simple expression,

$$p_{NB}(\rho) = (1 - f_s) \frac{P_{NB}}{V_p} H(\rho) \quad (15)$$

where P_{NB} is the injected NB power and f_s is the beam shinethrough. The fraction of this power that is deposited into the plasma electrons and ions, is calculated using the fast ion distribution function described in the following sections.

Neutral Beam Current Drive

The current driven by the fast ions as they slow down on the plasma electrons and ions on each flux surface ρ , is equal to,

$$J_f \approx \frac{\langle \mathbf{J} \cdot \mathbf{B} \rangle}{\langle B \rangle} = eZ_b \int d^3v \mathbf{v} \cdot \hat{\mathbf{b}} f_b(\mathbf{v}) \quad (16)$$

where Z_b is the atomic number of the beam species and $f_b(\mathbf{v})$ is the fast ion distribution function. In our model, the uniform field solution to the Fokker-Planck equation for the fast ions is used [9]. This formalism does not take into account the possible trapping of the fast ions, however this effect is expected to be small for tangential injection. It also neglects the beam current density due to energy diffusion of the fast ions. Accordingly $f_b(\mathbf{v})$ is given by,

$$f_b(\rho, v, \xi) = \frac{\dot{n}_f(\rho) \tau_s}{v^3 + v_c^3} \sum_{l=0}^{\infty} \frac{(2l+1)}{2} P_l(\xi) P_l(\xi_b) \left[\left(\frac{v^3}{v_b^3} \right) \left(\frac{v_b^3 + v_c^3}{v^3 + v_c^3} \right) \right]^{\frac{l(l+1)\hat{z}}{6}} \quad (17)$$

for $v \leq v_b$. In the above expression, $v_b = \sqrt{2E_b/m_b}$ is the initial velocity of the beam ions, v_c is the fast ion velocity corresponding to the critical energy for slowing down, $\xi = \cos \theta = (\mathbf{v}/v) \cdot \hat{\mathbf{b}}$, ξ_b is the initial pitch angle of the fast ions, and \hat{Z} is defined as,

$$\hat{Z} \equiv \frac{\sum_i n_i Z_i^2 \ln \Lambda_{bi}/A_b}{\sum_i n_i Z_i^2 \ln \Lambda_{bi}/A_i} \quad (18)$$

Standard expressions from the literature have been used to evaluate the various plasma parameters appearing above (collision times, Coulomb logarithms, critical slowing down energies, etc.). See for example references [10,11].

In terms of this fast ion distribution function, the fast ion current density is equal to,

$$J_f(\rho) = eZ_b \int_0^{v_b} dv \int_{-1}^1 d\xi v^3 \xi f_b(\rho, v, \xi) \quad (19)$$

which after carrying out the angular integration reduces to,

$$J_f(\rho) = eZ_b \dot{n}_f \tau_s \xi_b v_b I(y_c, \hat{Z}), \text{ where} \quad (20)$$

$$I(y_c, \hat{Z}) \equiv (1 + y_c^3)^{\hat{Z}/3} \int_0^1 dy \left[\frac{y^3}{y^3 + y_c^3} \right]^{\hat{Z}+1}$$

with $y = v/v_b$, and $y_c = v_c/v_b$. The integral I is evaluated numerically in the code at each flux surface ρ .

The fast ion current is partially canceled by the electron return current induced by the drag of the plasma electrons on the fast ions. This is modified in turn, when neoclassical electron trapping effects are taken into account. The net neutral beam driven current density is then,

$$J_{NB}(\rho) = \left\{ 1 - \frac{Z_b}{Z_{eff}} [1 - G(Z_{eff}, \epsilon)] \right\} \sum_{k=1}^3 J_{fk}(\rho) \quad (21)$$

where G is the trapped electron correction factor which has been calculated by Start and Cordey [12] for all aspect ratios and is approximated here by the parametric fit derived by Mikkelsen and Singer [10],

$$G(Z_{eff}, \epsilon) \approx \left(1.55 + \frac{0.85}{Z_{eff}} \right) \sqrt{\epsilon} - \left(0.20 + \frac{1.55}{Z_{eff}} \right) \epsilon \quad (22)$$

where $\varepsilon = \rho/R$, and the summation is over the three energy groups for positive ion beamlines. Once the net NB-driven current density is known, we can calculate the total NB current I_{NB} by integrating Eq. (21) over the plasma cross section, and the current drive efficiency $\eta_{NB} = I_{NB}/P_{NB}$ in A/W.

A final note regarding the calculation of the pitch angle at the birth of the fast ion, ξ_b that appears in the expression for the fast ion current density: Although simple analytic expressions for ξ_b exist in the literature [5], they tend to be invalid for the inner flux surfaces of the plasma. In the SUPERCODE Beams module, ξ_b is explicitly evaluated from:

$$\xi_b \equiv \langle \xi_b(\rho) \rangle = \sum_{\pm} \frac{\int dR_b \int dZ_b J_b(R_b, Z_b) h^{\pm}(\rho, R_b, Z_b) \frac{R_b}{R_{\pm}}}{\int dR_b \int dZ_b J_b(R_b, Z_b) h^{\pm}(\rho, R_b, Z_b)} \quad (23)$$

This evaluation of ξ_b using the above expression is very accurate as can be seen from Figure 2, where the average pitch angle is plotted as a function of ρ for different values of the tangency radius R_t using three different methods for calculating ξ_b : The analytic expression $\xi_b \approx R_t/(R_0 + \rho)$ [5], the expression given by Eq. 23 above, and using the Monte Carlo beam deposition code NFREYA [13]. It can be seen that our calculation is very close to the (accurate) result of NFREYA, while the analytic expression deviates for small ρ .

A few other fast ion quantities of interest are evaluated in the neutral beam module of the SUPERCODE:

Fast ion density:

The fast ion density is defined as,

$$n_b(\rho) = \int_0^{\infty} dv \int_{-1}^{+1} d\xi v^2 f_b(v, \xi) \quad (24)$$

and is equal to $n_b(\rho) = \dot{n}_f(\rho)\tau_f$ where τ_f is the fast ion lifetime,

$$\tau_f \equiv \frac{\tau_s}{3} \ln \left[\frac{1 + (v_b/v_c)^3}{1 + (v_{thi}/v_c)^3} \right] \quad (25)$$

The electron density contribution from the fast ion population needed for quasineutrality would then be equal to $Z_b n_b$.

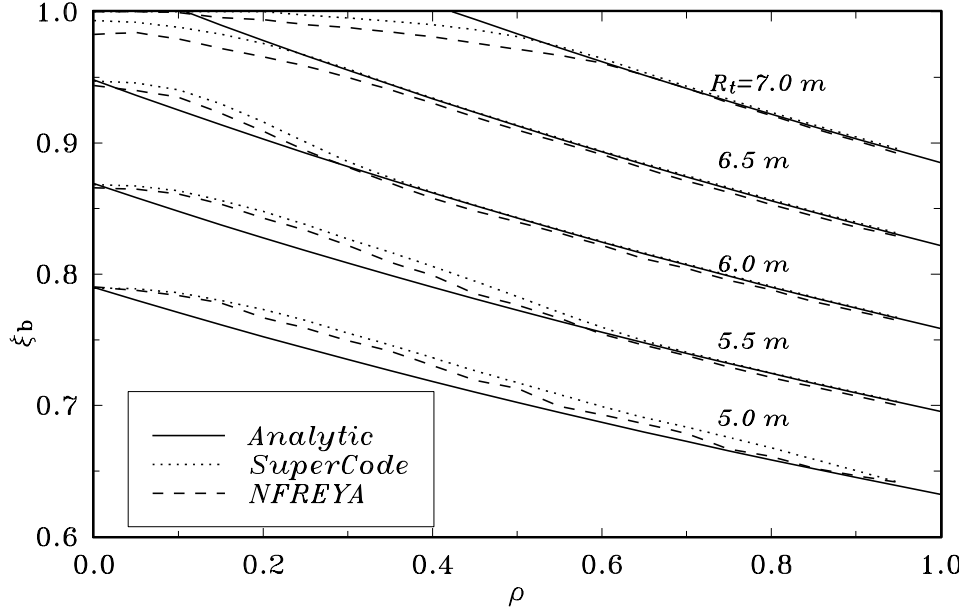


Figure 2: Average pitch angle for different tangency radii, evaluated with the analytic formula (solid line), the NB module of the SUPERCODE (dotted line), and the NFREYA code (dash line).

Fast ion pressure:

The fast ion pressure profile is useful for general MHD stability considerations as well as to assess the possibility of excitation of Toroidal Alfvén Eigenmodes (TAE's) by any super-Alfvénic beam ions. It is evaluated from its definition³,

$$p_b(\rho) \equiv \frac{m_b}{3} \int_0^{\infty} dv \int_{-1}^{+1} d\xi v^4 f_b(v, \xi) \quad (26)$$

Using the expression for the fast ion distribution function, we can express the fast ion pressure in an analytic form [14],

$$p_b(\rho) = \frac{m_b v_c^2 \tau_s \dot{n}_f(\rho)}{3} \left[\frac{x_c^2}{2} + \frac{1}{6} \ln \left(\frac{x_c^2 + 2x_c + 1}{x_c^2 - x_c + 1} \right) - \frac{1}{\sqrt{3}} \left\{ \tan^{-1} \left(\frac{2x_c - 1}{\sqrt{3}} \right) + \frac{\pi}{6} \right\} \right] \quad (27)$$

where v_c is the velocity corresponding to the critical energy for slowing down, and $x_c \equiv v_b/v_c$. Once the fast beam ion pressure profile is known, we can calculate the fast beam ion beta from,

³Note that this definition includes the dynamic pressure of the beam ions, since the fast ion distribution function is anisotropic.

$$\beta_b \equiv \frac{2\mu_0}{B_0^2} \frac{1}{V_p} \int d\rho V'(\rho) p_b(\rho) \quad (28)$$

Fractional Power Deposition:

The fraction of the NB heating power (Eq. 15) that is deposited to the plasma electrons and ions at each flux surface, is calculated by taking moments of the fast ion distribution function (Eq. 17). The fraction of the power going to the plasma ions is given by,

$$f_i(\rho) = \frac{2E_c(\rho)}{E_0} \int_0^{x_c(\rho)} dx \frac{x}{1+x^3} \quad (29)$$

where E_c is the critical energy for slowing down, E_b is the initial fast ion energy, and $x_c(\rho) = \sqrt{E_b/E_c(\rho)}$. This integral can be calculated analytically to give [14]:

$$f_i(\rho) = \frac{2}{x_c^2} \left[\frac{1}{\sqrt{3}} \left\{ \tan^{-1} \left(\frac{2x_c - 1}{\sqrt{3}} \right) + \frac{\pi}{6} \right\} - \frac{1}{6} \ln \left(\frac{x_c^2 + 2x_c + 1}{x_c^2 - x_c + 1} \right) \right] \quad (30)$$

The fraction of the NB power deposited into the electrons is then, $f_e = 1 - f_i$.

2.3. Beam-Target Interactions

As the fast beam ions slow down, they undergo fusion reactions with the background plasma ions. These beam-target interactions contribute to the total fusion power as well to the neutron production. The SUPERCODE Beams module can calculate the rates of several such reactions, their fusion power, and the resulting DT and DD neutron rates. The present version of the module includes contributions from $D(d, n)^3He$, $D(d, p)^3He$, $D(^3He, p)^4He$, and $D(t, n)^4He$ (if the relevant ion species are present in the plasma). The formulation allows for injection of either D or He , and the inclusion of the 3He reactions allows the study of $D - ^3He$ operating scenarios.

The calculation of the reaction rates for each reaction takes explicitly into account the slowing down distribution of the fast ions. It omits any contributions from beam-beam reactions, and the thermal motion of the background ions is neglected. Therefore,

$$RR(\rho) = n_i \int d^3v f_b(\mathbf{v}) v \sigma(v) \quad (31)$$

For the uniform field fast ion distribution function (Eq. 17), the reaction rate is equal to,

$$RR(\rho) \left(\frac{\#}{m^3 - s} \right) = \frac{n_i n_f(\rho) \tau_s}{\sqrt{2m_b}} \int_0^{E_b} \frac{\sigma(E) E^{-1/2} dE}{1 + \left(\frac{E_c}{E} \right)^{3/2}} \quad (32)$$

The energy integral is evaluated numerically in the module. Expressions for the different fusion cross sections $\sigma(E)$ involved, have been taken from the recent work by Hans-Stephan Bosch at IPP [15]. They are valid in the (center of mass) energy range from 0.5 keV to 5 MeV. This wide range allows us to model systems with present-technology neutral beams, up to next-generation devices with multi-MeV negative ion beams.

3. MODULE VERIFICATION

In this section we compare the predictions of the SUPERCODE neutral beam module with calculations from more sophisticated (but slower) codes such as the Monte Carlo deposition code NFREYA and the ACCOME neutral beam current drive code.

3.1. Comparisons with NFREYA⁴

NFREYA [13] is a Monte Carlo neutral beam deposition code widely used by the fusion community to model NB injection in tokamak plasmas. It can take into account the exact MHD flux surface geometry of the plasma, and it can model a variety of injection configurations and beam optics. For the purposes of the present comparison, the focal length of the NFREYA beams is taken to be infinite while the angular beam divergence is assumed to be zero. From the SUPERCODE part, the uniform power distribution option within the beam cross section is used. Both codes use the same routines for the calculation of the beam-stopping cross sections and share the same MHD geometry and plasma profiles generated by the SUPERCODE.

In Figure 3 the deposition profile, $H(\rho)$, is shown as calculated with the SUPERCODE Beams module and the NFREYA code, for a circular beam injected into an ITER plasma with parameters characteristic of the CDA ignition regime. The same comparison is repeated (Figure 4) using beams with rectangular cross section, like those of the ITER Reference Design [8]. Uniform power distribution is assumed.

From Figures 3 and 4, it can be seen that the agreement between the NFREYA code and the Beams module of the SUPERCODE is very good. Similar results have been obtained

⁴A similar comparison between FREYA (an older version of NFREYA for circular flux surfaces), and HOFER (a code based on the same model as our SUPERCODE module), has appeared before [16].

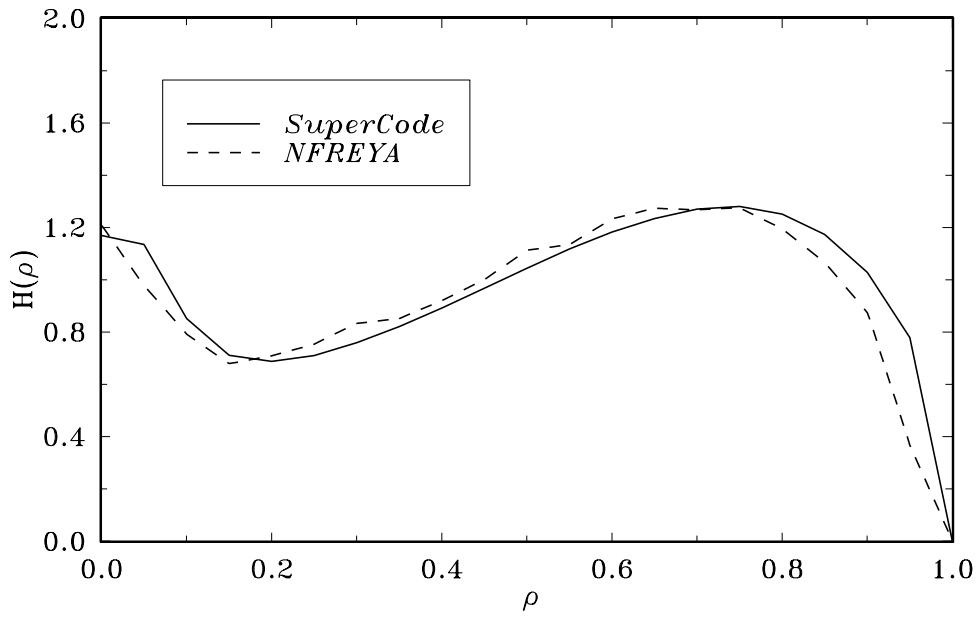


Figure 3: Comparison of the deposition profile for a circular beam calculated with the SUPERCODE (solid line) and NFREYA (dash line), for ITER CDA parameters.

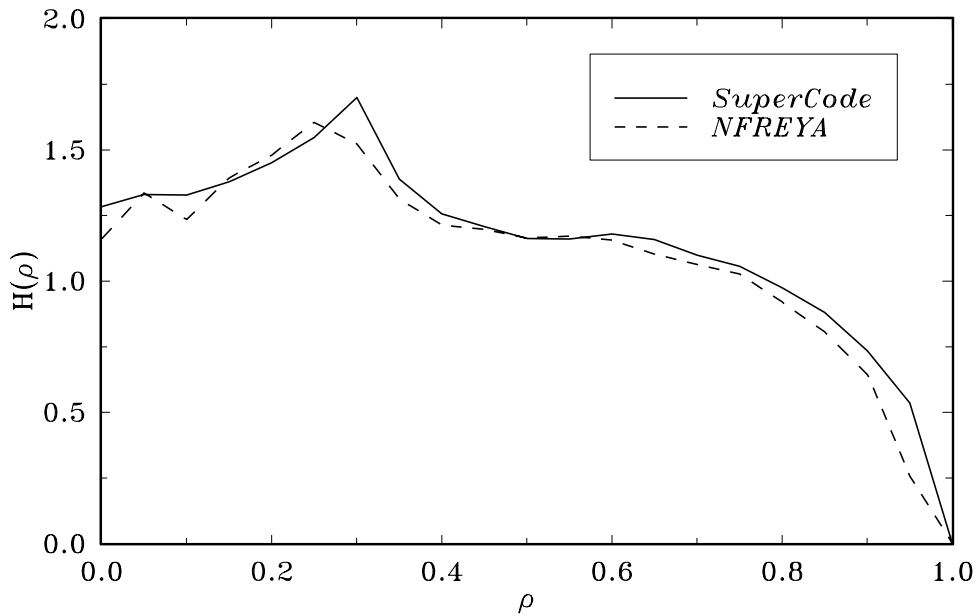


Figure 4: Comparison of the deposition profiles for a rectangular beam calculated with the SUPERCODE and NFREYA, for ITER CDA parameters.

for different injection and plasma parameters. It should also be mentioned that the execution time of NFREYA is at least an order of magnitude larger than that of our simple module.

The results presented above were for midplane injection with uniform power distribution within the cross section of the beam. However according to the ITER CDA reference neutral beam design [8], two of the three beamlines are injected at an angle above and below the midplane. Therefore, it is very important for the SUPERCODE Beams module to be able to model this type of injection. This is accomplished by using the bi-Gaussian power distribution (Eq. 11) with appropriate parameters for the vertical half-width σ_z , and the vertical position Z_s . Figure 5 demonstrates the sensitivity of the deposition profile to variations in the vertical position Z_s in Eq. 11 (keeping all the other relevant injection parameters constant), for the reference ITER CDA steady-state parameters.

So, it can be seen that the bi-Gaussian power distribution gives us enough flexibility to model off-midplane injection for cases (like the ITER CDA) where the injection is symmetric above and below the midplane. This approach has been used to benchmark our module against NB current drive simulations performed with the ACCOME code for the ITER CDA.

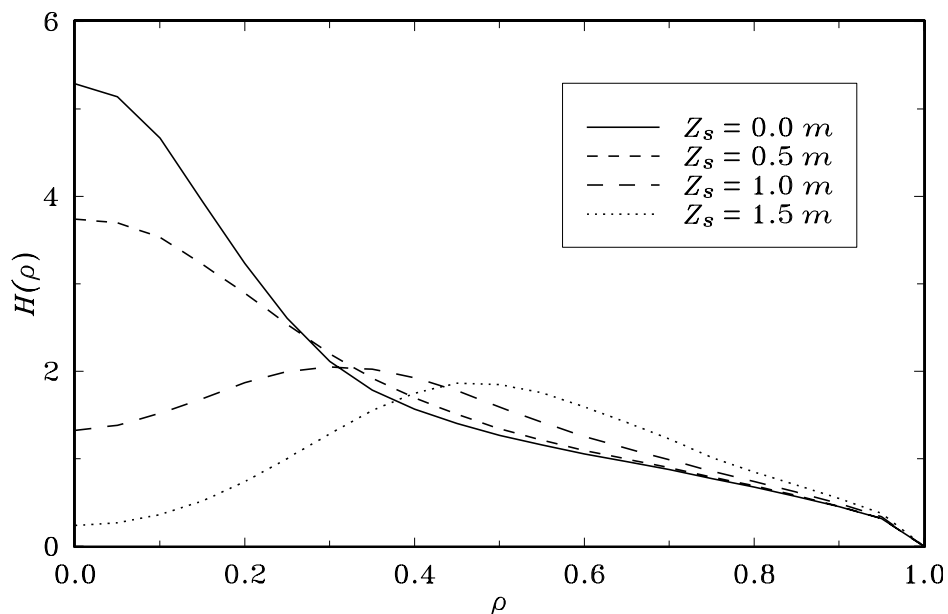


Figure 5: Sensitivity of the deposition profile to variations of the parameter Z_s (vertical position) of Eq. 11, for the reference ITER CDA steady-state parameters.

3.2. Comparisons with ACCOME

The predictions of the neutral beam module of the SUPERCODE have been compared with calculations performed with the ACCOME code [17] for an ITER CDA steady state case (actually case B6 in Ref. 18). To model the two beamlines that are injected at a vertical angle of $\pm 9.88^\circ$ above and below the midplane, the bi-Gaussian power distribution for rectangular beams (Eq. 11) is used. The two beamlines are modeled as one rectangular beam having a power equal to the sum of the powers of the two off-midplane injected beams (49.2 MW). The horizontal and vertical half-widths σ_R and σ_Z are taken equal to the horizontal and vertical $1/e$ half-radii of the reference design [17] (0.41 and 0.85 m respectively). The vertical position Z_S is taken equal to 1.4 m, a value giving the best agreement with the ACCOME deposition profile. The third beamline is lying on the midplane, so no special adjustments are necessary. The relevant input parameters for the SUPERCODE Beams module are summarized in the Table below:

Beamline	1	2
Energy (keV)	1300	1300
Power (MW)	49.6 (2×24.6)	29.6
Tangency radius, R_t (m)	6.2	6.2
Width, w (m)	1.00	1.00
Height, h (m)	4.00	4.00
σ_R (m)	0.41	0.41
σ_Z (m)	0.85	1.00
Z_S (m)	1.40	0.00

Table 1: Input parameters for the SUPERCODE Beams module, used in the benchmark with the ACCOME code for the Reference ITER CDA steady state scenario.

The results of the comparison are shown in Figure 6 where the net beam-driven current density (from all three beamlines) as computed by the two codes, is plotted as a function of the normalized poloidal flux. It can be seen that the agreement is quite good.

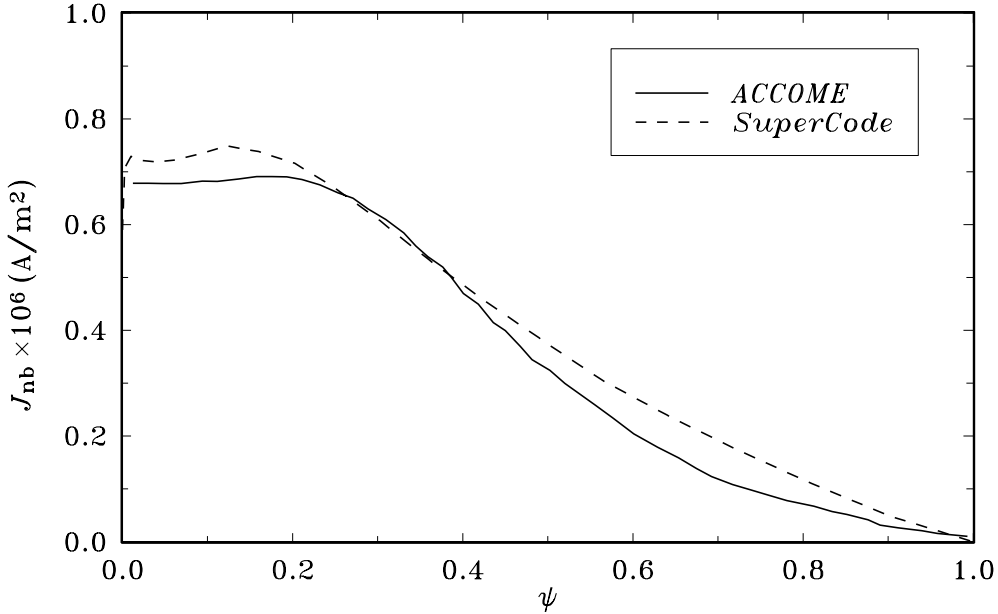


Figure 6: Comparison of the NB-driven current density, as calculated by ACCOME (solid line) and the SUPERCODE (dash line), for the reference ITER CDA steady-state scenario.

4. NUMERICAL CONSIDERATIONS

4.1. Numerical Methods

Since one of the most important considerations during the development of the neutral beam module for the SUPERCODE was computational speed, it is appropriate to include a brief description of the numerical methods used in the module. It is hoped that this discussion of the numerical techniques (which are otherwise ordinary), will help if further optimization of the module is desired, and will assist the user to make educated choices when adjusting input parameters for speed/accuracy trade-offs.

The calculation of the deposition profile $H(\rho)$ (Eq. 7) involves three integrations: A double integration on the surface of the beam (variables R_b, Z_b) and integrations along the beam path for the evaluation of the two beam attenuation integrals D_0 and D_1 . In addition, the solution of the nonlinear equation for the determination of ρ for a given R (Eq. 6) is required for each point along the beam path during the evaluation of D_0 and D_1 . Notice also that the integration along the beam path is inside the double

integration on the surface of the beam. A profiling of the code revealed that about 70% of the total computational time is spent for the evaluation of the integrals D_0 and D_1 . Unfortunately the accuracy of the integration along the beam path is very important for the overall accuracy of the profile calculation, since it is the only place where information about the plasma parameters enters the computation through the mean free path $\lambda(\rho)$. One may be tempted to make the assumption that $\lambda(\rho)$ is constant (not unreasonable, since the effective stopping cross section is not a very sensitive function of the plasma parameters), in which case $1/\lambda(\rho)$ can be taken outside the integration and the integral in Eq. (5) can be trivially calculated resulting to very significant savings on the total execution time. However, it was found that the resulting deposition profile calculated this way can have an error of more than 50%!

In the code, all these integrals are evaluated using standard Gaussian quadratures [19], according to the rule,

$$\int_a^b f(x)dx \approx \frac{b-a}{2} \sum_{i=1}^n w_i \sqrt{1-t_i^2} f(x_i) \quad (31)$$

where,

$$w_i = \frac{\pi}{n}, x_i = \frac{b-a}{2} t_i + \frac{b+a}{2}, \text{ and } t_i = \cos \frac{(2i-1)\pi}{2n} \quad (32)$$

The default number of nodes for the three integrals ($nr = nz = 6, ns = 8$) represents a conservative choice (error less than 1%) and can be reduced to improve speed, at some loss of accuracy.

For the solution of the nonlinear equation (6), an iterative method is used employing a correlated search algorithm [20]. This calculation accounts for about 50% of the total execution time (this is the most often-called routine of the program, being inside the innermost term in the triple integration for the evaluation of the deposition profile).

The calculations required for the evaluation of the different fast ion quantities (current, fusion reaction rates, etc.) involve integrations in the velocity space for each ρ (basically, the moments of the distribution function given by Eq. 17, as in Eqs. 19 and 30). These integrals are calculated using an adaptive Simpson's rule [20].

Finally, the calculations for the global quantities (total current, shinethrough, beta, total fusion powers, etc.) involve volume integrations that are performed using standard Gaussian quadratures.

4.2. Profiling of the code

A lot of insight can be gained regarding the numerical performance of a code if it is run through a profiler. In particular, it can help us identify the parts of the code where most of the execution time is spent. Fine-tuning these parts can result to large savings in the total execution time. Below, the results from a profiling session of the neutral beam module of the SUPERCODE are presented⁵.

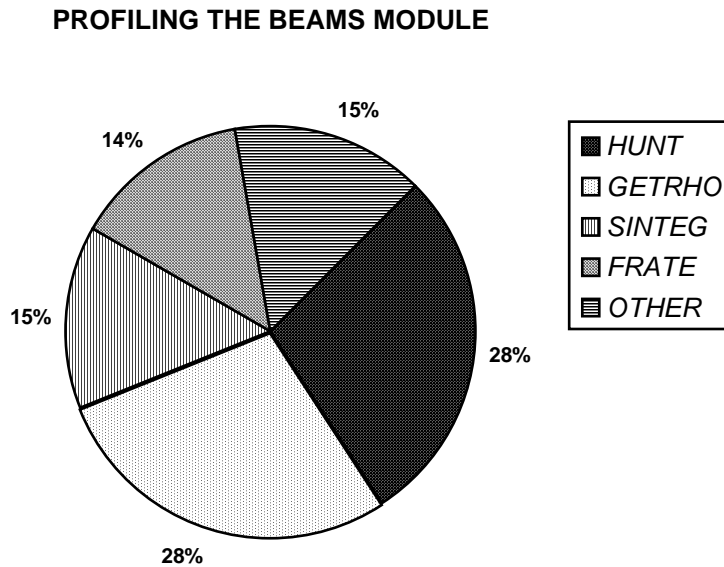


Figure 7: Percentage of the total execution time in the Beams module, for the top four routines. Only the time actually spent in the routine itself is taken into account, and not in any routines or functions that are called from the routine.

Several interesting conclusions can be drawn from the results of the profiling session: First, about 75% of the total execution time is spent in the calculation of the neutral beam deposition profile $H(\rho)$, and only 17.5% is spent in the evaluation of the fast ion quantities. This may appear excessive, however one should recall that all of the fast ion quantities depend on $H(\rho)$ in order to become profile-dependent. Most of the time for the calculation of $H(\rho)$ (about 71% of the total execution time) is actually spent calculating the integrals D_0 and D_1 (Eq. 5). Although great effort has been made to make the

⁵Actually, a stand-alone version of the module was used for the profiling. Therefore, some of the execution time included in the *OTHER* category involves activities not normally performed by the module when it is running as part of the SUPERCODE (I/O, generation of plasma and MHD profiles, etc).

routines that are involved in this part of the calculation (*SINTEG*, *GETRHO*, and *HUNT*) as efficient as possible, some room for improvement may still exist.

For the fast ion quantities, most of the time (14% of the total execution time) is spent inside the routine *FRATE* that calculates the fusion cross sections for the beam-target interactions. Since this routine evaluates the polynomial fits needed for the calculation of the fusion cross sections [15], not much can be done to increase its speed (at least if we want to retain the wide range of validity and high accuracy of the present fits). However, this routine is called during the velocity space integration, so any improvement in this part of the calculation could reduce the computational time. Alternatively, the calculation of the beam target interactions can be turned off through input action if they are not important for a particular simulation.

4.3. Cross-platform Benchmarks

A stand-alone version of the Beams module has been run in different hardware platforms to give us a quantitative idea of the module's speed. They included a CRAY-2 computer under UNICOS, a SPARCstation 2 (the main platform for the SUPERCODE), and a 486 25 MHz PC using the MS FORTRAN 5.1 compiler. For the purposes of this comparison, ten radial points were used and only one beamline. The results are shown in the graph below.

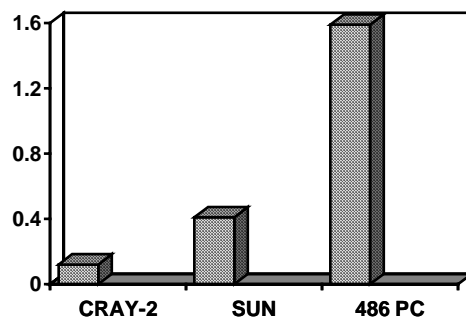


Figure 8: Execution time (s) of the Beams module for three different platforms.

It appears that 0.4 seconds are needed for a complete neutral beam calculation with one beamline, on the SPARCstation 2.

5. CONCLUSIONS

A neutral beam module has been developed for the needs of the SUPERCODE, the new fast 1-1/2 dimensional systems code for the ITER EDA and other tokamak design projects. The module can calculate self-consistently the profiles of most of the important NB-related parameters, including heating profiles, NB driven current, fast ion pressure, and fusion rates from beam-target interactions.

Although the module is computationally fast (0.4 seconds per run on a SPARCstation 2 workstation), very little sacrifice has been made in the accuracy of its physics models. Comparison of its predictions with results from more sophisticated codes reveals excellent agreement.

The neutral beam module allows us to use the SUPERCODE with confidence, for parametric systems studies of scenarios involving NB heating and current drive.

ACKNOWLEDGMENTS

This work was supported by the U.S. Department of Energy, under contract No. DE-FG05-91ER54122.

REFERENCES

- 1 S. W. Haney, et al. *A "SuperCode" for Performing Systems Analysis of Tokamak Experiments*, to be presented at the ANS meeting, 1992.
- 2 G.G Lister, D.E Post, and R. Goldston, "Computer Simulation of Neutral Beam Injection into Tokamaks Using Monte Carlo Techniques," *Third Symposium on Plasma Heating in Toroidal Devices*, Varenna, Italy (1976) 303.
- 3 J. A. Rome, J.D. Callen, and J.F. Clarke, "Neutral Beam Injection into a Tokamak: Fast Ion Spatial Distribution for Tangential Injection," *Nucl. Fusion* **14**, 141 (1974).
- 4 S.E. Attenberger, W.A. Houlberg, and S.P. Hirshman, "Some Practical Considerations Involving Spectral Representations of 3D Plasma Equilibria," *Journal of Comp. Phys.* **72**, 435 (1987).
- 5 H.C. Howe, *Physics Models in the Tokamak Transport Code PROCTR*, Oak Ridge National Laboratory Report ORNL/TM-9537, (1985).
- 6 R.K. Janev, C.D. Boley, and D.E. Post, "Penetration of Energetic Neutral Beams into Fusion Plasmas," *Nucl. Fusion* **29**, 2125 (1989).
- 7 C.D. Boley, *private communication*, 1989.
- 8 V. Parail, et al., *ITER Current Drive and Heating System*, ITER Documentation Series, No. 32, IAEA, Vienna 1991.
- 9 J.D. Gaffey, "Energetic Ion Distribution Resulting from Neutral Beam Injection in Tokamaks," *J. Plasma Physics* **16**, 149 (1976).
- 10 D.R. Mikkelsen, and C.E. Singer, "Optimization of Steady-State Beam-Driven Tokamaks of Arbitrary Aspect Ratio," *Nuclear Technology/Fusion* **4** 237 (1983).
- 11 D.L. Book, *NRL Plasma Formulary*, Washington, DC 1990.
- 12 D.F.H. Start, and J.G. Cordey, "Beam-induced Currents in Toroidal Plasmas of Arbitrary Aspect Ratio," *Phys. Fluids* **23**, 1477 (1980).
- 13 R.H. Fowler, J.A. Holmes, and J. A. Rome, *NFREYA - A Monte Carlo Beam Deposition Code for Noncircular Tokamak Plasmas*, Oak Ridge National Laboratory Report ORNL/TM-6845, (1979).
- 14 B.Q. Deng and G.A. Emmert, *Fast Ion Pressure in Fusion Plasmas*, UWFD-718 (1987).

- 15 H.S. Bosch, "Review of Data and Formulas for Fusion Cross-sections," *Max-Planck-Institut für Plasmaphysik Report*, **IPP I/252**, September 1990.
- 16 R.M. Wieland, W.A. Houlberg, and A.T. Mense, *A Comparison of Beam Deposition for Three Neutral Beam Injection Codes*, Oak Ridge National Laboratory Report ORNL/TM-6550, (1979).
- 17 M.E. Fenstermacher, *private communication*, 1991.
- 18 D.E. Post, J. Wesley, L.J. Perkins, and J.D. Galambos, *ITER Operation Scenarios*, ITER/US/91/PC-06-2
- 19 M. Abramowitz, and I. A. Stegun, *Handbook of Mathematical Functions*, NY (1970).
- 20 W.H. Press, *et al.*, *Numerical Recipes*, Cambridge (1986).

